Cureus
Part of SPRINGER NATURE

Open Access Case Report

Diagnostic Impact of Integrated Molecular Testing in Nodal T-follicular Helper Cell Lymphoma Mimicking Castleman Disease and Classic Hodgkin Lymphoma: A Report of Two Cases

Review began 07/16/2026
Review ended 10/30/2026
Published 11/08/2026

© **Copyright** 2026
Shah et al. This is an open access article distributed under the terms of the Creative Commons Attribution License CC-BY 4.0., which permits unrestricted use, distribution, and reproduction in any medium, provided the original author and source are credited.

DOI: 10.7759/cureus.119325

Bhaumik Shah [1], Mitra Abdolahi [2], Fahad Ahmed [3], Rashmi Khanal [3], Reza Nejati [1]

1. Pathology/Hematopathology, Fox Chase Cancer Center, Philadelphia, USA 2. Pathology, Mayo Clinic Comprehensive Cancer Center, Jacksonville, USA 3. Pathology, Fox Chase Cancer Center, Philadelphia, USA

Corresponding author: Reza Nejati, reza.nejati@fccc.edu

Abstract

Nodal T-follicular helper cell lymphoma (nTFHL) has a broad morphologic spectrum and can closely mimic Castleman disease (CD) and classic Hodgkin lymphoma (CHL), particularly in limited biopsies and when flow cytometry is noncontributory. We report two diagnostically challenging cases in which the diagnosis was established by integrating histopathology, T-follicular helper (TFH) immunophenotyping, T-cell receptor (TCR) clonality testing, and targeted next-generation sequencing (NGS). Case 1 was a 64-year-old woman whose excisional lymph node biopsy showed regressed germinal centers, prominent high endothelial venules (HEVs), and hyalinized “lollipop” vessels resembling CD. Initial immunohistochemistry and flow cytometry were noncontributory. Clonal TCR gene rearrangement, NGS demonstrating DNMT3A R882H and two TET2 mutations (variant allele frequencies 26-33%), and subsequent TFH-marker staining established nTFHL with Castleman-like features. CD30 positivity (>20%) supported selection of brentuximab vedotin-based systemic therapy. Case 2 was an 82-year-old man with previously treated follicular lymphoma whose supraclavicular core biopsy contained CD30-positive Hodgkin/Reed-Sternberg (HRS)-like cells, initially suggesting CHL. Clonal TCR rearrangement, RHOA G17V, multiple TET2 variants (variant allele frequencies 36-44%), and a CTCF splice-site variant supported angioimmunoblastic-type nTFHL. Chromosomal microarray analysis (CMA), performed only in this case, showed complex genomic imbalances and was supportive rather than required for diagnosis. The patient completed six cycles of brentuximab vedotin, cyclophosphamide, doxorubicin, and prednisone with a complete metabolic response and remains in remission on observation. These cases illustrate a practical stepwise approach: Castleman-like nodal architecture with focal atypia, or HRS-like cells in a T-cell-rich background, should prompt TFH immunophenotyping and TCR clonality testing. Targeted NGS can be added in selected inconclusive cases. TET2 and DNMT3A mutations and TCR clonality alone are not independently diagnostic. Comprehensive molecular testing is most useful when conventional evaluation is insufficient, rather than as a routine first-line approach.

Categories: Hematology, Pathology, Oncology
Keywords: castleman disease pathophysiology, classic hodgkin lymphoma, next-generation dna sequencing, nodal t-follicular helper cell lymphoma, peripheral t-cell lymphoma angioimmunoblastic

Introduction

T-follicular helper (TFH) cells are a CD4-positive T-cell subset that normally resides in germinal centers and supports B-cell maturation through costimulatory molecules and cytokines, including PD-1, ICOS, CXCL13, and IL-21. Nodal TFH lymphoma (nTFHL) is the umbrella term used in the World Health Organization 5th Edition (WHO-5) and the International Consensus Classification (ICC) for mature T-cell lymphomas of TFH derivation. This family includes angioimmunoblastic-type nTFHL (nTFHL-AI), historically termed angioimmunoblastic T-cell lymphoma (AITL); follicular-type nTFHL; and nTFHL, not otherwise specified (NOS). Diagnosis requires compatible nodal architecture plus expression of at least two, and preferably three, TFH-associated markers (PD-1, ICOS, CXCL13, CD10, BCL6, and, where available, CXCR5), interpreted in the clinical and molecular context.

nTFHL typically shows a polymorphous infiltrate of lymphocytes, eosinophils, plasma cells, histiocytes, and immunoblasts. Classic architectural clues include perinodal infiltration with relative sparing of subcapsular sinuses, high endothelial venule (HEV) proliferation, and extrafollicular follicular dendritic cell (FDC) expansion. These features are often incomplete in core biopsies. Two recurring mimics make routine sign-out particularly difficult. First, large CD30-positive cells that resemble Hodgkin/Reed-Sternberg (HRS) cells may prompt a diagnosis of classic Hodgkin lymphoma (CHL), especially mixed-cellularity or lymphocyte-rich subtypes [1-6]. Second, hyalinized vessels, regressed germinal centers, and FDC expansion may suggest Castleman disease (CD), a nonclonal lymphoproliferative disorder that includes unicentric and multicentric

How to cite this article
Shah B, Abdolahi M, Ahmed F, et al. (November 08, 2026) Diagnostic Impact of Integrated Molecular Testing in Nodal T-follicular Helper Cell Lymphoma Mimicking Castleman Disease and Classic Hodgkin Lymphoma: A Report of Two Cases. Cureus 18(11): e119325. DOI 10.7759/cureus.119325

forms and, in a subset of multicentric disease, HHV-8 association [7]. “Castleman-like” change can also be secondary to an underlying lymphoma and should not be equated with primary CD without exclusion of a T-cell neoplasm [7,8].

TFH immunophenotyping and T-cell receptor (TCR) clonality testing are the essential next steps when morphology is ambiguous. Recurrent mutations in TET2, DNMT3A, RHOA, and IDH2 are enriched in nTFHL and are uncommon in CHL [8], but TET2 and DNMT3A alterations also occur in age- and therapy-related clonal hematopoiesis and are not, by themselves, diagnostic of lymphoma. Targeted next-generation sequencing (NGS) and, in selected cases, chromosomal microarray analysis (CMA) can support the diagnosis when immunohistochemistry is partial, or the biopsy is limited; they do not replace morphology and phenotype.

Accurate distinction among nTFHL, CHL, and CD changes treatment. We report two cases that illustrate this problem: nTFHL with Castleman-like architecture and nTFHL-AI mimicking CHL on a core biopsy. In both, the diagnosis required integration of histology, a qualifying TFH immunophenotype, TCR clonality, and supportive molecular findings rather than any single test.

Case Presentation

Here, we present two cases of nTFHL with unusual histologic features and challenging differential diagnoses in which molecular studies played a crucial role in establishing the final diagnosis, underscoring the critical role of advanced molecular techniques in modern hematopathology, particularly for resolving ambiguous or borderline cases where conventional diagnostic methods may fall short.

Case 1

A 64-year-old woman with a history of anal squamous cell carcinoma treated with chemoradiotherapy presented with recurrent fevers, fatigue, and progressively enlarging lymphadenopathy. Physical examination showed palpable cervical and axillary lymphadenopathy. Serial FDG-PET/CT scans demonstrated widespread FDG-avid multistation lymphadenopathy involving cervical, mediastinal, axillary, abdominal, and pelvic nodes (Figure *1*), with representative maximum standardized uptake values in the 7.4-8.6 range, raising concern for lymphoma. An initial left axillary core biopsy showed only reactive changes. During this interval, she developed elevated inflammatory markers (erythrocyte sedimentation rate (ESR) >100 mm/h and markedly increased C-reactive protein (CRP)), hypergammaglobulinemia (IgG up to 2,850 mg/dL) with an IgG-kappa band on serum protein electrophoresis, elevated β2-microglobulin (3.39 mg/L), and intermittent steroid responsiveness. HIV-1/2 antigen/antibody screen and HHV-8 were negative. Eastern Cooperative Oncology Group (ECOG) performance status was 1. One year after the nondiagnostic core biopsy, persistent FDG-avid lymphadenopathy prompted right axillary lymph node excision. Pretreatment bone marrow biopsy showed cellular marrow with trilineage hematopoiesis and involvement by clonal kappa-restricted plasmacytoid B cells.

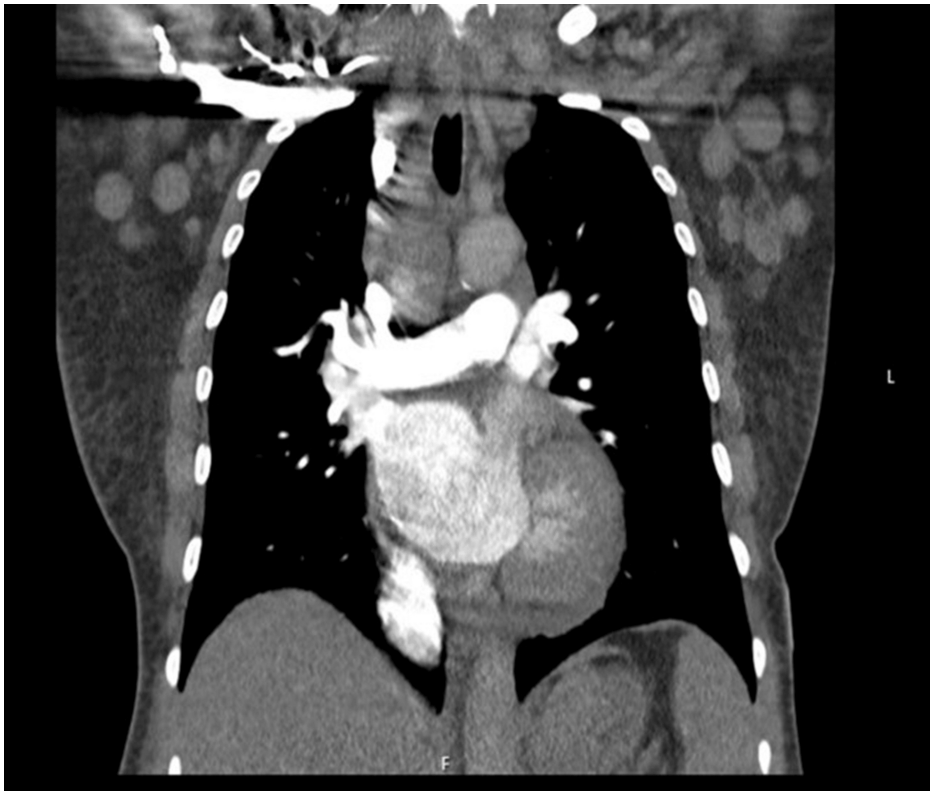


FIGURE 1: PET/CT imaging (case 1)

PET/CT: positron emission tomography/computed tomography; FDG: fluorodeoxyglucose

PET/CT imaging in case 1 demonstrating extensive FDG-avid cervical, mediastinal, axillary, and para-aortic lymphadenopathy, raising concern for an underlying lymphoma

The excisional biopsy showed altered nodal architecture with regressed germinal centers, increased follicular dendritic cells (FDCs), twinned follicles, prominent HEVs, and hyalinized "lollipop" vessels reminiscent of CD (Figures *2A*-*2D*). Atypical large lymphoid cells were present in interfollicular areas. Flow cytometry did not identify an aberrant T- or B-cell population. Initial immunohistochemistry for routine T- and B-cell markers showed no definite neoplastic phenotype. CD21 highlighted only very focal disruption of the FDC meshwork. Epstein-Barr virus-encoded RNA (EBER) in situ hybridization was positive in scattered cells, a finding recognized in nTFHL-AI and insufficient by itself for an EBV-positive B-cell lymphoproliferative disorder. Plasma EBV DNA PCR was not detected.

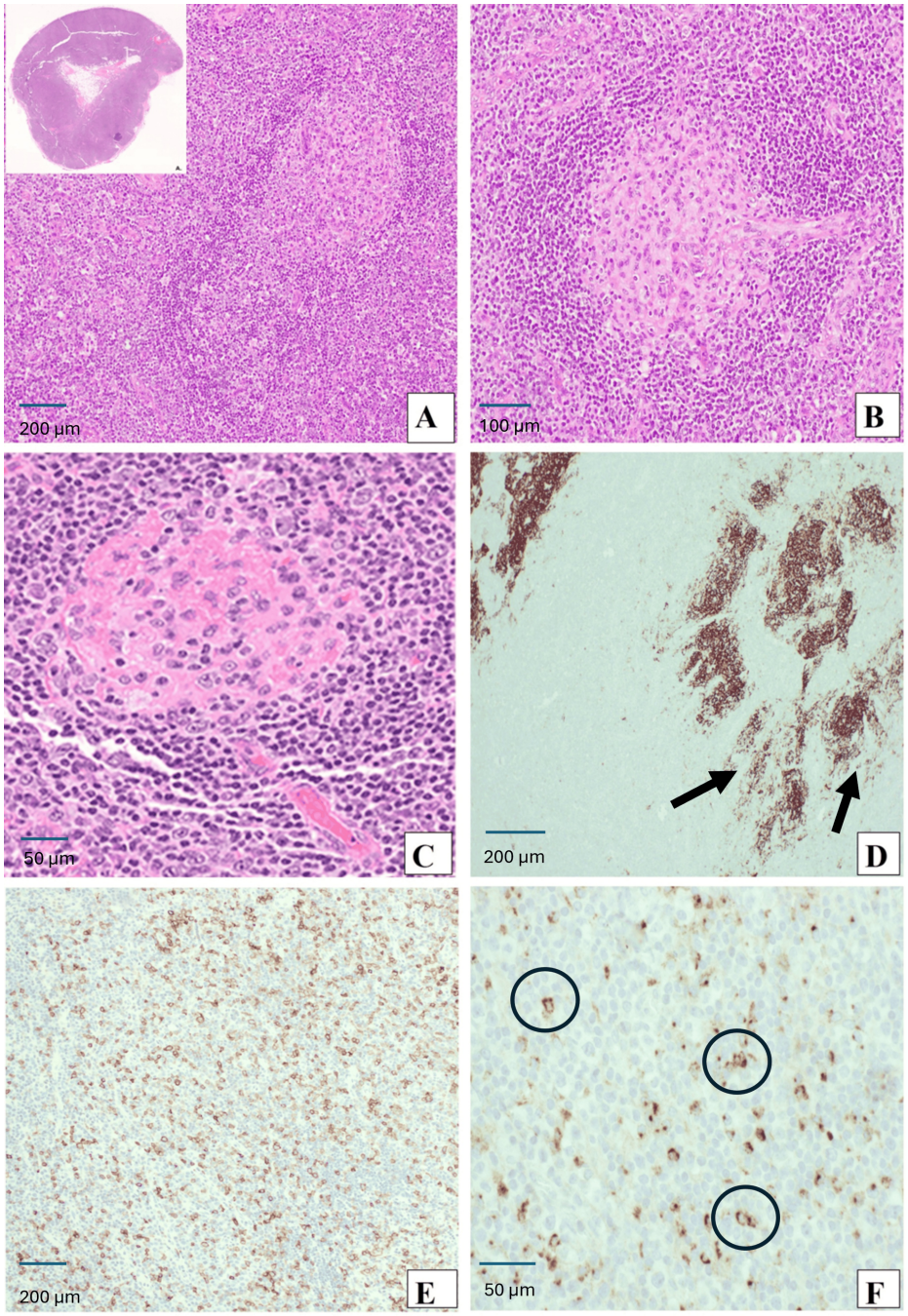


FIGURE 2: Histopathological features of an enlarged lymph node with Castleman-like changes (case 1)

TFH: T-follicular helper; FDC: follicular dendritic cell

(A) Low-power view (4× objective; inset) showing preserved nodal architecture with an intact capsule and markedly expanded follicles with occasional "twinning" (closely apposed germinal centers separated by a thin rim of mantle zone cells; scale bar = 200 µm). (B) "Onion-skinning" of mantle zone lymphocytes concentrically arranged around a hyalinized vessel (10× objective; scale bar = 100 µm). (C) Higher-power view of a regressed germinal center with a hyalinized penetrating vessel ("lollipop" lesion; 20× objective; scale bar = 50 µm). (D) CD21 highlights an expanded FDC meshwork with focal extrafollicular expansion of dendritic cells (arrows; 4× objective; scale bar = 200 µm). (E) ICOS immunostaining highlights increased TFH cells within and outside the disrupted FDC meshwork (4× objective; scale bar = 200 µm). (F) CXCL13 positivity confirms the presence of TFH cells within Castleman-like areas (circles; 20× objective; scale bar = 50 µm)

Molecular studies detected clonal T-cell receptor (TCR) beta and gamma gene rearrangements. Targeted NGS (275-gene panel) identified DNMT3A p.Arg882His (variant allele frequency (VAF) 32.6%), TET2 p.His1219Arg (VAF: 30.6%), and TET2 splice-site variant c.4182+1G>C (VAF: 26.0%). IDH2 was not reported

as altered. These TET2 and DNMT3A variants are enriched in nTFHL but are also common in clonal hematopoiesis, particularly in older patients with prior cytotoxic therapy, and were interpreted only in combination with morphology, immunophenotype, and TCR clonality. A B-cell gene rearrangement study showed a clonal IGK light-chain signal with a polyclonal IgH background; this was interpreted as an emerging B-cell subclone rather than a coexisting B-cell lymphoma.

On the basis of the clonality result, additional immunohistochemistry was performed and demonstrated a focally expanded extrafollicular population of TFH cells coexpressing CD4, ICOS, PD-1, and CXCL13 (Figures *2E*-*2F*), with retained CD5 and CD7. CD30 was positive in >20% of the atypical lymphoid cells. Expression of four TFH-associated markers in the appropriate architectural context fulfilled WHO-5/ICC immunophenotypic criteria for nTFHL (⩾2 TFH markers, preferably ⩾3). Combined with HEV prominence and extrafollicular FDC expansion, the findings were classified as nTFHL, nTFHL-AI, with Castleman-like features, Lugano stage IVB (fever as a B symptom; no documented extranodal organ involvement).

After diagnosis, the patient received six cycles of brentuximab vedotin, cyclophosphamide, doxorubicin, and prednisone (BV-CHP). CD30 positivity supported the choice of a brentuximab-containing regimen. Treatment was tolerated through cycle 3. The patient was subsequently followed at an outside institution; no further follow-up data are available from our records.

Case 2

An 82-year-old man with follicular lymphoma, WHO grade 1-2 of 3, diagnosed in November 2020 and treated with eight weekly doses of rituximab with a complete metabolic response, presented with bulky thoracic, upper abdominal, mesenteric, and retroperitoneal lymphadenopathy on CT, suggesting progressive lymphoma. ECOG performance status was 0. HIV-1/2 antigen/antibody screen was nonreactive, and HHV-8 was negative.

A supraclavicular lymph node core-needle biopsy yielded small fragments of atypical lymphoid tissue with a mixed infiltrate of small to medium-sized lymphocytes, scattered plasma cells and histiocytes, and rare large atypical mononuclear and multinucleated Hodgkin-like cells with prominent eosinophilic nucleoli (Figures *3A*-*3B*). By immunohistochemistry, the large cells were positive for PAX5, CD30, MUM1, OCT2, BOB1, and BCL6 (Figures *3C*-*3D*) and negative for CD3, CD10, CD15, CD20, and ALK. Flow cytometry showed no clonal B-cell population and no immunophenotypically abnormal T-cell population. Given the limited core and CD30-positive large cells, CHL was the leading consideration. Recurrent follicular lymphoma and histologic transformation were considered but were not supported by the absence of a follicular B-cell architecture, CD20-negative large cells, and lack of a clonal B-cell population by flow cytometry.

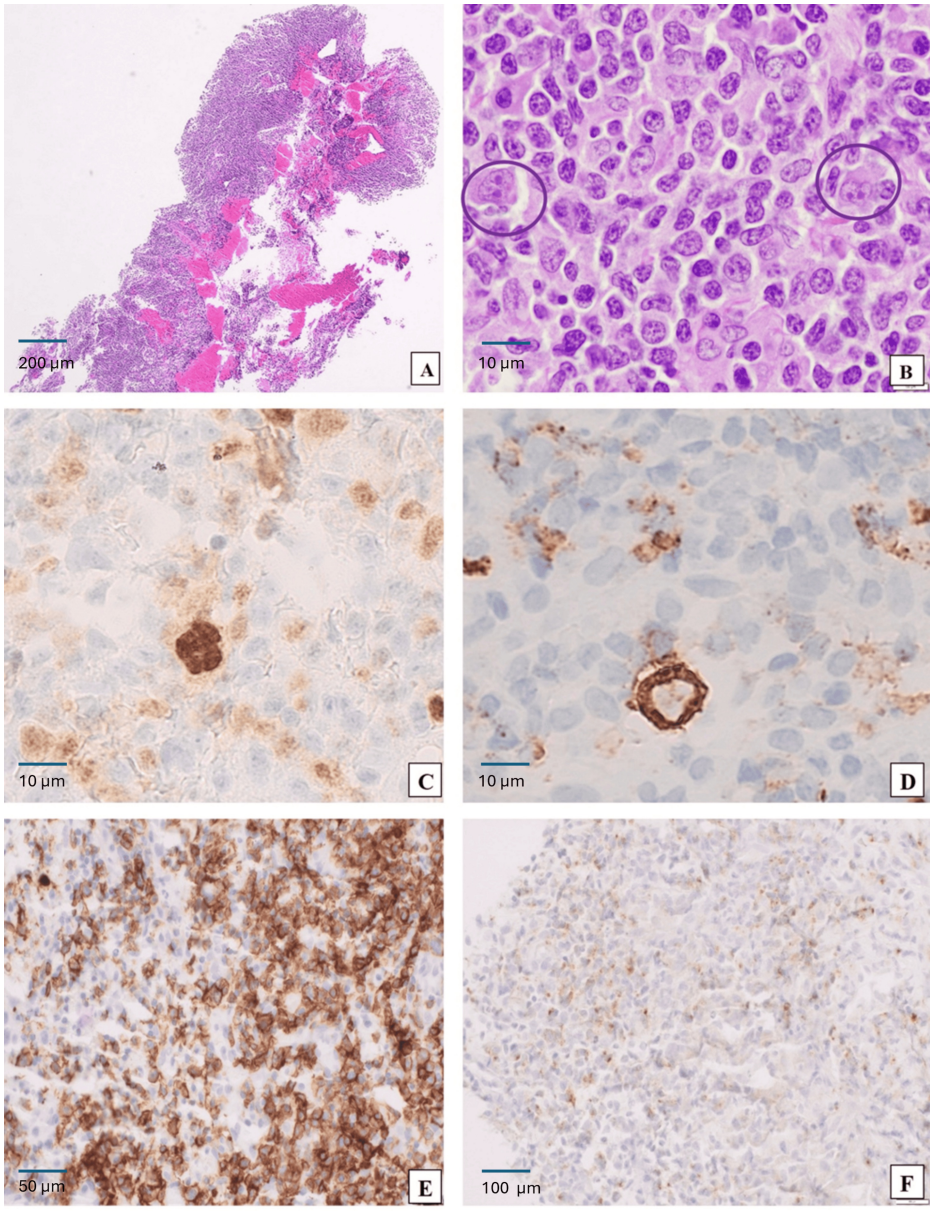


FIGURE 3: Histologic and immunophenotypic features of the lymph node core biopsy (case 2)

TFH: T-follicular helper; HRS: Hodgkin/Reed-Sternberg

(A) Low-power view (4× objective) showing small core fragments of lymphoid tissue with a polymorphous infiltrate (scale bar = 200 µm). (B) High-power view (60× objective) revealing a mixed cellular infiltrate composed of small to medium-sized lymphocytes, plasma cells, and histiocytes, with rare large atypical mononuclear and multinucleated HRS-like cells (circles; scale bar = 10 µm). (C) MUM1 immunohistochemistry highlighting nuclear positivity in the large atypical cells (60× objective; scale bar = 10 µm). (D) CD30 immunostain strongly labeling HRS-like cells (60× objective; scale bar = 10 µm). (E) ICOS immunostaining demonstrating an expanded background population of TFH cells (20× objective; scale bar = 50 µm). (F) CXCL13 immunostaining confirming TFH cells (10× objective; scale bar = 100 µm)

Molecular studies demonstrated a clonal TCR gamma gene rearrangement. Targeted NGS (275-gene panel) identified RHOA p.Gly17Val (c.50G>T; VAF: 32.1%), two TET2 variants (p.Val415fs; c.1243delG; VAF: 35.8% and p.Leu446*; c.1337T>G; VAF: 44.2%), and a CTCF splice-site variant (c.782-2A>G; VAF: 7.1%). IDH2 was not reported as altered. CMA showed multiple genomic imbalances, including losses at 4q, 6q, 20q, and Y, and copy-neutral loss of heterozygosity (cnLOH) at 12q in approximately 60% of cells (Figure *4*). Additional immunohistochemistry for ICOS and CXCL13 highlighted an expanded TFH-cell population in the background (Figures *3E*-*3F*). Expression of at least two TFH-associated markers, clonal TCR, and RHOA G17V in this morphologic setting fulfilled WHO-5/ICC criteria for nTFHL-AI. The TET2 variants were interpreted as supportive but not specific, given the patient's age and prior therapy and the possibility of

clonal hematopoiesis. CMA provided corroborative evidence of a complex neoplastic genome and was not required to establish the diagnosis. Disease was staged as Lugano IVB.

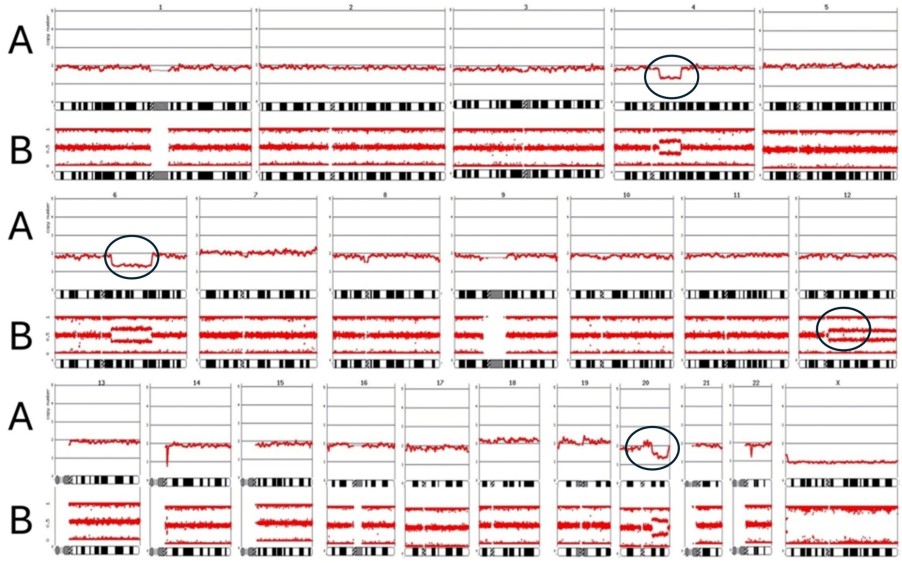


FIGURE 4: CMA profile from case 2 demonstrating complex genomic abnormalities supporting the diagnosis of nTFHL-AI

CMA: chromosomal microarray analysis; nTFHL-AI: angioimmunoblastic-type nodal T-follicular helper lymphoma

(A) Copy-number track (log2 ratio, upper panels) and (B) B-allele frequency track (lower panels) across chromosomes 1–22 and X. Circles highlight the key abnormalities: losses at 4q, 6q, and 20q (copy-number track) and copy-neutral loss of heterozygosity at 12q (B-allele frequency track). Loss of the Y chromosome was also present but is not shown. Normal B-allele frequency profiles show three bands; loss or splitting of the middle band indicates loss of heterozygosity. The x-axis depicts genomic coordinates; the y-axis of the upper track depicts DNA copy number, and the lower track depicts B-allele frequency. These complex genomic imbalances support a neoplastic process and were corroborative but not required for the diagnosis of nTFHL-AI

The patient completed six cycles of brentuximab vedotin, cyclophosphamide, doxorubicin, and prednisone (BV-CHP) from March to June 2023, with good tolerance. CD30 positivity of the large cells supported use of a brentuximab-containing regimen. End-of-treatment FDG-PET/CT showed a complete metabolic response (Deauville 1). As of October 2026, more than three years after completion of therapy, the patient remains under observation with no clinical or radiographic evidence of lymphoma recurrence. Subsequent FDG-avid bone lesions were biopsy-proven to represent metastatic prostate cancer rather than relapsed nTFHL. He continues to have stable chronic anemia and thrombocytopenia attributed to comorbidities.

Discussion

These two cases show how nTFHL can reproduce the architecture of CD or the cytology of CHL, and why the diagnosis depends on integration of histology, a qualifying TFH immunophenotype, TCR clonality, and supportive molecular data rather than any single result [1,3,8]. TET2 and DNMT3A mutations, detected in both cases, are not specific for nTFHL. They are also the most common drivers of age- and therapy-related clonal hematopoiesis, and both patients were older and had prior cytotoxic exposure. NGS was performed on bulk lymph-node tissue without cell sorting. Those variants were therefore interpreted only together with morphology, TFH marker coexpression meeting WHO-5/ICC criteria (≥2 TFH markers, preferably ≥3), and clonal TCR rearrangement [8,9]. TCR clonality alone would also have been insufficient, because clonal TCR rearrangements can occur in reactive T-cell expansions.

Castleman-like change is a recognized mimic and, in a minority of patients first labeled as CD, the node is later reclassified as lymphoma or another neoplasm [7,10]. In true CD, the hyaline-vascular or plasma-cell alterations are diffuse and dominate the node. In lymphoma-associated Castleman-like reactions, the same features are often focal, and cytologic atypia, an aberrant T-cell phenotype, or clonal TCR rearrangement is present [7,11,12]. Case 1 followed that pattern: lollipop vessels and regressed germinal centers suggested CD, but focal FDC disruption, extrafollicular TFH cells coexpressing ICOS, PD-1, and CXCL13, clonal TCR, and co-occurring TET2 and DNMT3A variants established nTFHL-AI with Castleman-like features. RHOA G17V was absent, which does not exclude nTFHL; RHOA G17V is found in only about half to two-thirds of cases [8,13]. Scattered EBER-positive cells were regarded as the EBV-positive B-immunoblast expansion typical of nTFHL-AI after loss of T-cell immune surveillance, not as a standalone EBV-positive B-cell

lymphoproliferative disorder, which was excluded by T-cell clonality and the TFH phenotype of the atypical T cells. HHV-8 and HIV were negative.

Other considerations with Castleman-like or mixed nodal architecture include reactive TFH hyperplasia, peripheral T-cell lymphoma, not otherwise specified (PTCL-NOS), EBV-positive polymorphic B-cell lymphoproliferative disorder, IgG4-related lymphadenopathy, Rosai-Dorfman disease, FDC sarcoma, and reactive follicular hyperplasia. Reactive TFH hyperplasia lacks a clonal TCR and architectural effacement. PTCL-NOS lacks a qualifying TFH phenotype. IgG4-related disease and Rosai-Dorfman disease have distinctive plasma-cell ratios or S100-positive emperipolesis, which were absent. FDC sarcoma forms a spindle-cell neoplasm, not a TFH-rich T-cell lymphoma.

Case 2 illustrates the CHL mimic. CD30-positive, PAX5-dim large cells in a T-cell-rich core biopsy frequently lead to an initial CHL diagnosis [1-3,14-16]. Features against CHL were an expanded ICOS+/CXCL13+ TFH background, clonal TCR gamma rearrangement, RHOA G17V (VAF: 32.1%), and two truncating TET2 variants (VAFs 35.8% and 44.2%). RHOA G17V is more lineage-restricted than TET2 and, at a VAF similar to the higher TET2 calls, supports a neoplastic TFH clone rather than incidental clonal hematopoiesis of indeterminate potential (CHIP) alone [8,14]. The low-VAF CTCF splice-site variant (7.1%) is of uncertain contribution. CMA showed losses at 4q, 6q, 20q, and Y and cnLOH at 12q; these complex imbalances favor a neoplastic genome over a purely reactive or isolated CHIP process, but CMA was supportive and was not required for diagnosis. Recurrent follicular lymphoma and transformation were considered because of the prior grade 1-2 follicular lymphoma treated with rituximab. They were not supported by the lack of a follicular B-cell neoplasm, CD20-negative large cells, and the absence of a clonal B-cell population by flow cytometry.

Flow cytometry was noncontributory in both cases. Neoplastic TFH cells may be few, lose surface CD3, or be lost in fibrotic or core-biopsy material. A negative flow study does not exclude nTFHL and should not delay tissue-based TFH immunohistochemistry and TCR testing.

A practical sequence, acknowledging that large NGS panels and CMA are not available in every laboratory, is as follows. First, perform a TFH marker panel (PD-1, ICOS, CXCL13, CD10, and BCL6) plus CD30 and EBER when Castleman-like change with focal atypia, or HRS-like cells in a T-cell-rich background, is present. Second, add TCR clonality if morphology or phenotype is incomplete. Third, use targeted NGS when the combined histology, phenotype, and clonality remain inconclusive, or when CHIP versus lymphoma must be considered in an older or previously treated patient. Fourth, reserve CMA for selected cases with limited tissue and a still-open differential after NGS. The minimum work-up that would have prevented misclassification in these two cases is TFH immunohistochemistry plus TCR clonality; NGS added confidence, and CD30 positivity supported selection of BV-CHP in both patients.

These observations come from two cases and should not be read as a mandate for comprehensive molecular testing in every TFH-rich node. Case 2 remains in remission more than three years after completing therapy, while longer follow-up is limited for case 1. The findings support a low threshold to consider nTFHL before defaulting to CD or CHL when the architecture is incomplete, the biopsy is small, or flow cytometry is negative.

Conclusions

nTFHL can closely mimic CD and CHL, especially in limited biopsies and when flow cytometry is negative. In these two cases, the diagnosis was established by integrating histology, a qualifying TFH immunophenotype, and TCR clonality, with targeted NGS used as support. CMA was performed only in case 2 and was corroborative, not required. Molecular results helped confirm nTFHL and, once the diagnosis and CD30 status were established, informed selection of systemic therapy; they do not replace conventional work-up and are not indicated in every TFH-rich node. When Castleman-like architecture with focal atypia, or HRS-like cells in a T-cell-rich background, is encountered, TFH immunohistochemistry and TCR clonality testing should precede a default diagnosis of CD or CHL. Targeted NGS can be added if that combination remains inconclusive or if clonal hematopoiesis must be distinguished from lymphoma. TET2 and DNMT3A variants and TCR clonality are not independently diagnostic. This report is limited to two retrospectively identified cases. Follow-up remains limited for case 1, whereas case 2 has remained in remission more than three years after completing therapy. Access to large NGS panels and microarray analysis varies by institution. These observations therefore support a selective, stepwise approach rather than routine comprehensive molecular testing.

Additional Information

Author Contributions

All authors have reviewed the final version to be published and agreed to be accountable for all aspects of the work.

Concept and design: Bhaumik Shah, Reza Nejati, Fahad Ahmed, Mitra Abdolahi, Rashmi Khanal

Acquisition, analysis, or interpretation of data: Bhaumik Shah, Reza Nejati, Fahad Ahmed, Mitra Abdolahi, Rashmi Khanal

Drafting of the manuscript: Bhaumik Shah, Reza Nejati, Fahad Ahmed, Mitra Abdolahi, Rashmi Khanal

Critical review of the manuscript for important intellectual content: Bhaumik Shah, Reza Nejati, Rashmi Khanal

Supervision: Reza Nejati

Disclosures

Human subjects: Informed consent for treatment and open access publication was obtained or waived by all participants in this study. Fox Chase Cancer Center, Philadelphia issued approval Not applicable. Data obtained from routine clinical care; no research study conducted. **Conflicts of interest:** In compliance with the ICMJE uniform disclosure form, all authors declare the following: **Payment/services info:** All authors have declared that no financial support was received from any organization for the submitted work. **Financial relationships:** All authors have declared that they have no financial relationships at present or within the previous three years with any organizations that might have an interest in the submitted work. **Other relationships:** All authors have declared that there are no other relationships or activities that could appear to have influenced the submitted work.

Acknowledgements

The biospecimens and retrospective clinical, molecular, and cytogenomic data presented in both cases were obtained as part of routine patient care. All ancillary studies, including chromosomal microarray analysis and next-generation sequencing, were performed for diagnostic purposes per standard institutional protocols, not specifically for this study. No additional specimens or data were collected. This work complies with Fox Chase Cancer Center Institutional Review Board ethical guidelines and HIPAA standards; the presented material contains no identifiable information or unique characteristics that could directly or indirectly identify the patients.

References

1. Moroch J, Copie-Bergman C, de Leval L, et al.: Follicular peripheral T-cell lymphoma expands the spectrum of classical Hodgkin lymphoma mimics. Am J Surg Pathol. 2012, 36:1636-46. 10.1097/PAS.0b013e318268d9ff
2. Sakakibara A, Suzuki Y, Kato H, et al.: Follicular T-cell lymphoma mimicking lymphocyte-rich classic Hodgkin lymphoma: a case report of a diagnostic pitfall. J Clin Exp Hematop. 2021, 61:97-101. 10.3960/jslrt.20052
3. Nicolae A, Pittaluga S, Venkataraman G, Vijnovich-Baron A, Xi L, Raffeld M, Jaffe ES: Peripheral T-cell lymphomas of follicular T-helper cell derivation with Hodgkin/Reed-Sternberg cells of B-cell lineage: both EBV-positive and EBV-negative variants exist. Am J Surg Pathol. 2013, 37:816-26. 10.1097/PAS.0b013e3182785610
4. Eladl AE, Satou A, Elsayed AA, Suzuki Y, Kato S, Asano N, Nakamura S: Clinicopathological study of 30 cases of peripheral T-cell lymphoma with Hodgkin and Reed-Sternberg-like B-cells from Japan. Am J Surg Pathol. 2017, 41:506-16. 10.1097/PAS.0000000000000813
5. Xie Y, Jaffe ES: How I diagnose angioimmunoblastic T-cell lymphoma . Am J Clin Pathol. 2021, 156:1-14. 10.1093/ajcp/aqab090
6. Gomez-Gelvez JC, Smith LB: Reed-Sternberg-like cells in non-Hodgkin lymphomas . Arch Pathol Lab Med. 2015, 139:1205-10. 10.5858/arpa.2015-0197-RAI
7. Zhang X, Niyazi S, Guo H, Zhang L: Mimickers and associated neoplasms of Castleman disease . J Clin Transl Pathol. 2025, 5:20-9. 10.14218/JCTP.2024.00047
8. Dobay MP, Lemonnier F, Missiaglia E, et al.: Integrative clinicopathological and molecular analyses of angioimmunoblastic T-cell lymphoma and other nodal lymphomas of follicular helper T-cell origin. Haematologica. 2017, 102:e148-51. 10.3324/haematol.2016.158428
9. Oksenhendler E, Boutboul D, Fajgenbaum D, et al.: The full spectrum of Castleman disease: 273 patients studied over 20 years. Br J Haematol. 2018, 180:206-16. 10.1111/bjh.15019
10. Nakazato Y, Tsuchida S, Takada-Owada A, et al.: Castleman disease and mimickers: clinicopathological findings of atypical lymphoproliferative disorders associated with autoimmune disease. J Clin Exp Hematop. 2022, 62:119-26. 10.3960/jslrt.22025
11. Fajgenbaum DC, Uldrick TS, Bagg A, et al.: International, evidence-based consensus diagnostic criteria for HHV-8-negative/idiopathic multicentric Castleman disease. Blood. 2017, 129:1646-57. 10.1182/blood-2016-10-746933
12. Odejide O, Weigert O, Lane AA, et al.: A targeted mutational landscape of angioimmunoblastic T-cell lymphoma. Blood. 2014, 123:1293-6. 10.1182/blood-2013-10-531509
13. Zheng J, Wang Z, Pan X, et al.: DNMT3A(R882H) accelerates angioimmunoblastic T-cell lymphoma in mice . Oncogene. 2023, 42:1940-50. 10.1038/s41388-023-02699-2
14. Scourzic L, Couronné L, Pedersen MT, et al.: DNMT3A(R882H) mutant and Tet2 inactivation cooperate in the deregulation of DNA methylation control to induce lymphoid malignancies in mice. Leukemia. 2016, 30:1388-98. 10.1038/leu.2016.29
15. Petronilho S, Poullot E, Andre A, et al.: Follicular helper T-cell lymphoma with Hodgkin/Reed-Sternberg-like cells versus classic Hodgkin lymphoma: a comparative study. Am J Surg Pathol. 2025, 49:273-83.

10.1097/PAS.0000000000002345

16. Alikhan M, Song JY, Sohani AR, et al.: Peripheral T-cell lymphomas of follicular helper T-cell type frequently display an aberrant CD3(-/dim)CD4(+) population by flow cytometry: an important clue to the diagnosis of a Hodgkin lymphoma mimic. Mod Pathol. 2016, 29:1173-82. 10.1038/modpathol.2016.113